Available online at www.sciencedirect.com
ScienceDirect
Trans. Nonferrous Met. Soc. China 28(2018) 273−281
Transactions of Nonferrous Metals Society of China
www.tnmsc.cn

Microstructural evolution and mechanical properties of Ti−5Al−5Mo−5V−3Cr alloy by heat treatment with continuous temperature gradient

Sheng-hang XU, Yong LIU, Bin LIU, Xin WANG, Zhi-xing CHEN

State Key Laboratory of Powder Metallurgy, Central South University, Changsha 410083, China

Received 24 November 2016; accepted 2 August 2017

Abstract: A new high throughput heat-treatment method with a continuous temperature gradient between 600 and 700 °C was utilized on the Ti-5553 alloy (Ti−5Al−5Mo−5V−3Cr, mass fraction, %). The temperature gradient was induced by the variation of the axial section of sample, which was heated by the direct current. The variation of continuous cooling rates on the treated sample was realized by using the end quenching method. The microstructural evolution and mechanical properties under different heat treatment conditions were evaluated. The results show that the pseudo-spinodal decomposition of the alloy occurs at (617±1) °C, and the size of the precipitated α phase is around 300 nm. Moreover, the highest microhardness is obtained after the heat treatment at the pseudo-spinodal decomposition temperature for 4 h. These indicate that the high throughput method is efficient and fast to determine the phase transformation temperature and corresponding microstructural evolution of alloys.

Key words: Ti−5Al−5Mo−5V−3Cr alloy; high throughput method; pseudo-spinodal decomposition; temperature gradient; microstructure; mechanical properties

1 Introduction

Near-β titanium alloys, which can be quenched to room temperature and retain a full β phase microstructure, are wildly used in structural applications. Ti-5553 alloy (Ti−5Al−5Mo−5V−3Cr, mass fraction, %) is one kind of new near-β titanium alloys with excellent hardenability and reduced sensitivity of hot working variables [1]. It has gradually replaced Ti−10V−2Fe−3Al and Ti−6Al−4V in the applications of landing gear of Boeing-787 and Airbus-A380 airplanes. However, the optimization of mechanical properties, such as balancing strength, toughness, ductility and fatigue resistance, is dependent on very careful control of the thermo-mechanical processing parameters. A little change in processing parameters can induce very different precipitation microstructures and properties [1−3]. For near-β titanium alloys, the high strength is usually controlled not only by the β phase itself, but also largely by the distribution of the fine-scaled α precipitates [4]. IVASISHIN et al [5] studied three near-β titanium alloys, TIMETAL-LCB, VT22 and Ti-15-3-3-3 (Ti-15-3), and found that only fine plate-like α lathes contribute to high strength. It is most likely that the fine α phase induces a large number of α/β interfaces, which hinder the movement of dislocations.

Recently, a new non-classical strengthening mechanism in β-Ti alloys called pseudo-spinodal decomposition has been discovered [6]. The mechanism favors thermodynamically in the transformation of β phase into fine α phase without compositional change but involving compositional fluctuations [7,8]. The microstructure, presenting a chessboard nanowire structure, is very sensitive to temperature as well as alloy composition [9]. This decomposition was observed in other alloys like Co−Pt [10], Ti−Nb−Al [11] and even in some oxide ceramics [12−14]. In Ti alloys, the pseudo-spinodal decomposition of Timetal 21S alloy (Ti−15Mo−3Al−2.7Nb−0.3Si, mass fraction, %) was studied. The results indicated that the pseudo-spinodal decomposition became active at 550 °C, leading to a drastic increase in the density of intragranular α precipitates. Ti-5553 alloy was also studied by NAG et al [8], and the temperature of pseudo-spinodal decomposition was found to be between 600 and 650 °C. However, the exact

Foundation item: Project (2014CB644002) supported by the National Basic Research and Development Project of China; Project (2015CX004) supported by the Innovation-driven Plan in Central South University, China
Corresponding author: Yong LIU; Tel: +86-731-88830406; E-mail: yonliu@csu.edu.cn
DOI: 10.1016/S1003-6326(18)64660-6

temperature was not determined yet. Therefore, there are also some uncertainties in the pseudo-spinodal decomposition of Ti-5553 alloy. Firstly, it is very time-consuming in observing the microstructural change of the alloy aged at very small temperature intervals in order to determine the accurate temperature for the pseudo-spinodal decomposition. Secondly, since the mechanical properties are largely dependent on the size and volume fraction of α phase, it is very important to systematically study the microstructural evolution in the pseudo-spinodal decomposition. Currently, there have been some high throughput methods for studying the compositional designs and microstructural evolution of alloys. These methods can also be used to optimize process parameters in a time-saving and efficient way. AFONSO et al [15] utilized the end quenching test to obtain different cooling rates of Ti−20Nb alloy. The variation of cooling rates leads to different microstructures and mechanical properties.

In this work, a new high throughput heat treatment method was developed. In this method, a temperature gradient was exerted on the samples. Each section of the sample represented a heat treatment condition, and the microstructural evolution in the whole temperature range can be conveniently studied by using a single sample. The method was used to study the pseudo-spinodal decomposition of Ti-5553 alloy, in order to determine the accurate decomposition temperature and to build up the relationship between the heat treatment parameters and the precipitation of α phase.

2 Experimental

2.1 Material preparation

The forged Ti-5553 alloy used in the present work was provided by Baogang Company, China. The chemical composition of the alloy is shown in Table 1.

Table 1 Chemical composition of Ti-5553 alloy (mass fraction, %)

Al	Mo	V	Cr	Fe	O	N	Ti
5.57	4.97	4.93	3.05	0.49	0.145	0.02	Bal.

Small circular truncated cone sample with the length of 40 mm shown in Fig. 1(a) was cut from the Ti-5553 alloy bar by spark erosion, and then encapsulated in quartz tube under the protection of pure argon. The sample was heated to 1000 °C for 1 h to produce a full β-phase microstructure with equiaxed grains. After that, the sample was equipped on the Gleeble3180 thermal mechanical machine and then heated by the direct current, and the local heat was dependent on the electric resistance of the Ti-5553 alloy, shown as follows:

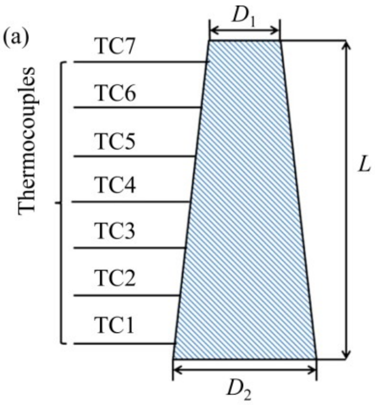

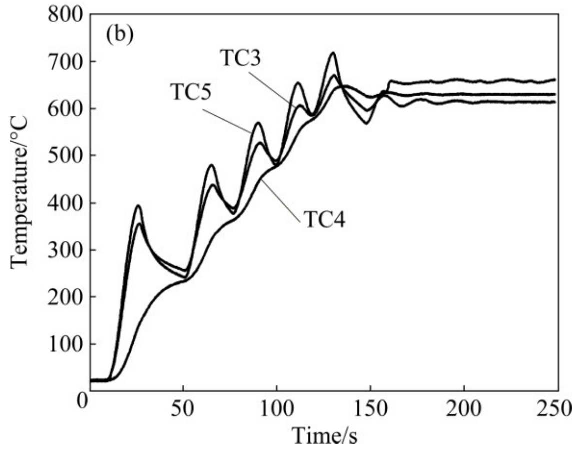

Fig. 1 Schematic illustration of sample for high throughput heat-treatment method (a) and temperature change with heating time measured by thermocouples (b)

$$Q=I^2Rt \tag{1}$$

where Q denotes the thermal energy, I is the current, R represents the resistance of the Ti-5553 alloy and t is the time. The resistance of the alloy is decided as follows:

$$R=\frac{\rho L}{s} \tag{2}$$

where ρ is the electrical resistivity of Ti-5553 alloy, L and s denote the length and the cross-sectional area of the sample, respectively, and ρ is a function of temperature which can be defined by

$$\rho=\rho_0(1+\alpha T) \tag{3}$$

where ρ_0 is the electrical resistivity at 0 °C, α denotes the coefficient of resistance to temperature and T represents the temperature. Finally, the thermal energy can be described according to the above equations as

$$Q=\frac{I^2\rho_0(1+\alpha T)Lt}{s} \tag{4}$$

So, it is clear that the energy received through the current thermal effect at different positions is dependent on the cross-sectional area of the sample. The change of the cross-sectional area is continuous, leading to the continuous temperature gradient under the electric current heating. Besides, the heat radiation effect is also taken into consideration, which is dependent on the surface temperature of the sample. When the radiating heat energy is equal to the current thermal effect energy, the temperature of the surface keeps stable with the time extending. In this experiment, sustained and stable continuous temperature gradient can be achieved under the certain current. In order to measure the accurate temperature, thermocouples were positioned in seven different regions with interval distance of 5 mm. Then, the sample was heated in vacuum by the electric current with a heating rate of 40 °C/min to the appropriate temperatures measured between 600 and 700 °C, and held for different time (30 min, 1 h, 4 h and 20 h). The temperature was steady during the aging progress monitored by the thermocouples shown in Fig. 1(b). The fast cooling rate was realized by filling argon in the Gleeble chamber. In this way, a continuous temperature gradient between 600 and 700 °C on a single sample was produced.

The end quenching test was also used to produce continuous cooling rates on the samples, and the method was reported in Ref. [16]. Firstly, the samples with size of 4 mm × 4 mm × 40 mm were heated to 1000 °C for 1 h to obtain the full β-phase microstructure. Then, the samples were heated to 617 °C with a rapid heating rate of 40 °C/min, and held for 1 h, followed by immersing one end of the samples into the water and keeping the other side in air until the whole samples were cooled to room temperature. The end quenching test was carried out to investigate the influence of the cooling rate on the pseudo-spinodal decomposition.

2.2 Material characterization

The microstructures were observed by using a Leica optical microscope (OM) and an FEI Nova Nano230 scanning electron microscope (SEM), and the transmission electron microscopy (TEM) measurement was conducted in an FEI Tecnai20 instrument at 200 kV. After sectioning, metallographic samples were ground, polished, and then etched with a solution of 10% HF, 5% HNO_3 and 85% H_2O (in volume). The samples for TEM observation were prepared by mechanical milling on different emery papers to a thickness of 50−80 μm, and then by ion milling. The phase identification was performed on bulk samples using a D/max-2550VB X-ray diffraction analyzer at 45 kV and 40 mA and room temperature.

The Vickers hardness of the alloy was measured at 16 different places with aging temperature range from 600 to 680 °C. An IBIS nanoindentation tester equipped with a Berkovich diamond indenter was operated at a maximum load of 50 mN.

3 Results

3.1 Evolution of microstructures with aging temperature

The sample directly water quenched from the solution treatment at 1000 °C for 1 h exhibits a single β phase microstructure, with large equiaxed grains of about 250 μm in size, as shown in Fig. 2(a). XRD pattern in Fig. 2(b) also reveals the only existence of β-phase in the alloy.

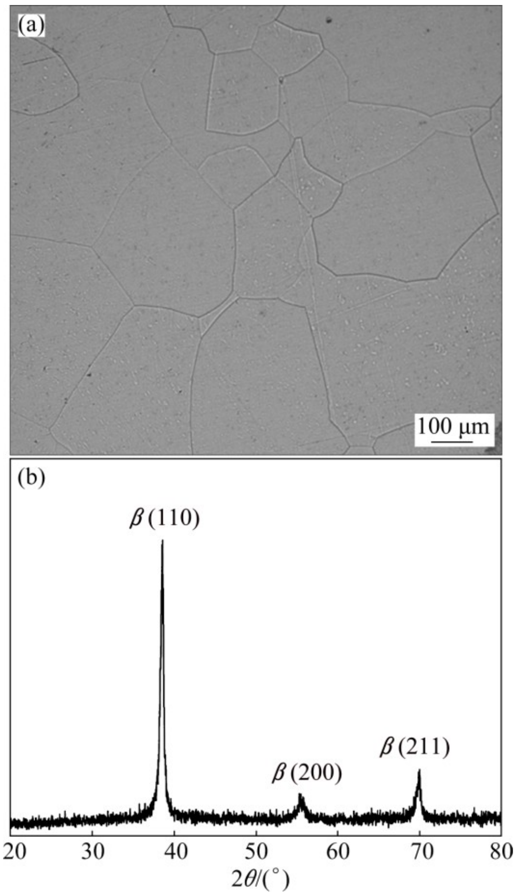

Fig. 2 Optical microstructure (a) and XRD pattern (b) of Ti-5553 alloy after solution treatment at 1000 °C for 1 h

Figure 3 shows the microstructures of the samples after aging with a temperature gradient for 1 h. The temperature at different positions can be calculated by the parabola calculation in different temperature intervals.

When the pseudo-spinodal decomposition in Ti-5553 alloy occurs, a drastic increase in the density of intergranular α precipitates with an ultra-fine size can be detected [8]. It can be seen that aging at (617±1) °C shows the finest α phase with a length size of 300 nm in Fig. 4(a), while that aging at 640 °C is about 5 μm, as shown in Fig. 4(b). Then, α phase becomes fine again at 660 °C with a length size of 1 μm, as shown in Fig. 4(c).

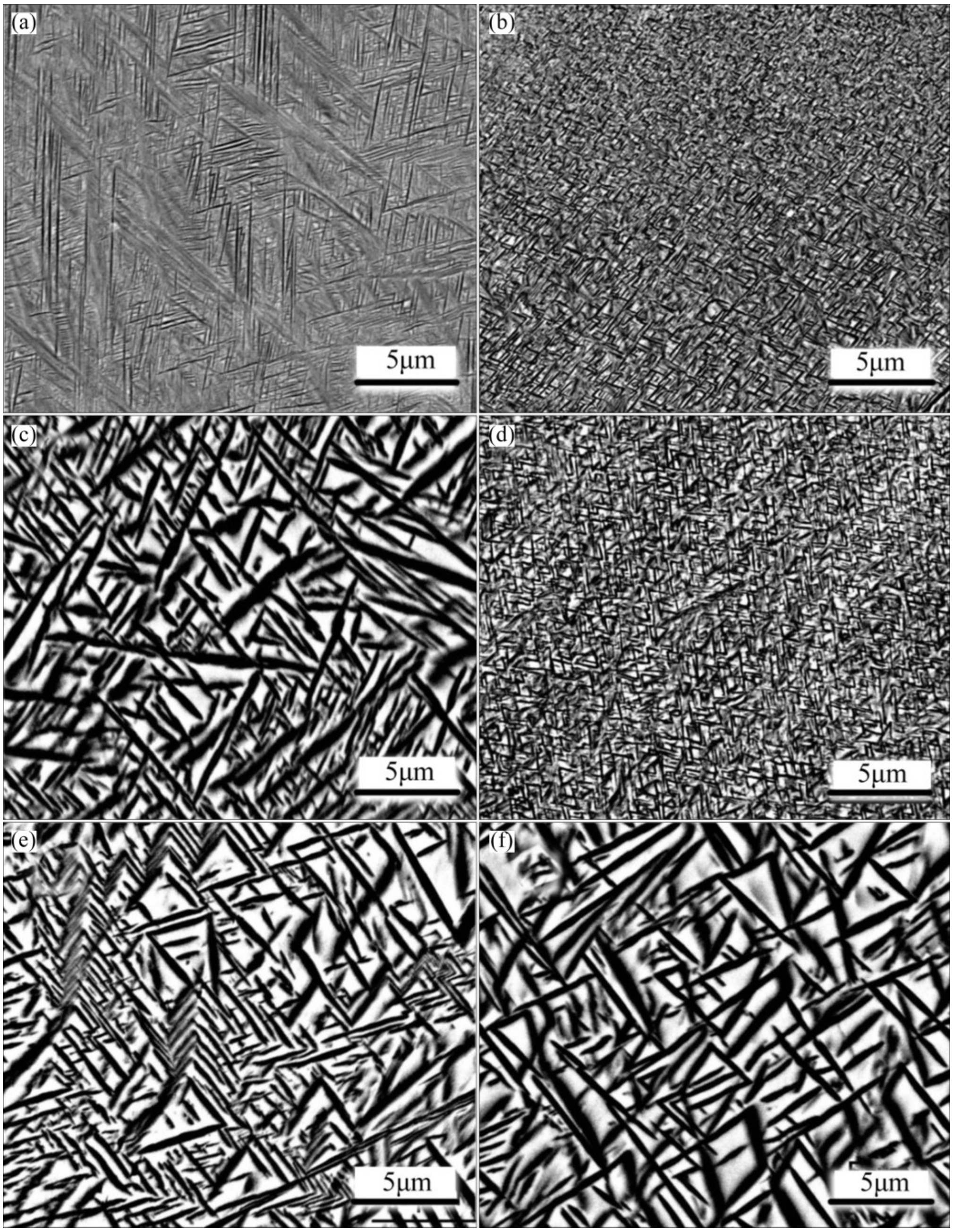

Fig. 3 Microstructures of Ti-5553 alloy after heat treatment with continuous temperature gradient for 1 h: (a) 600 °C; (b) 617 °C; (c) 640 °C; (d) 660 °C; (e) 680 °C; (f) 700 °C

The temperature is close to the nose temperature of the TTT (time−temperature−transformation) curve of Ti-5553 alloy [17]. At this temperature, a large number of α particles precipitate, but the growth can be restricted by adjacent nuclei. Actually, the precipitated α phase intersects with each other in Figs. 3(e) and 4(c). When aging at a high temperature of 680 °C, the length size of α phase is more than 10 μm, as shown in Fig. 3(e).

3.2 Evolution of microstructures with aging time

Figure 5 shows the microstructures of Ti-5553 samples aged at 640 °C for different time from 30 min to 4 h. Plate-like α phase can be obviously seen in the β matrix in different orientations.

Figure 6 illustrates the relationship between volume fraction of α phase and the aging temperature for different time. The volume fraction of α phase, which was measured by Image Tool software through more than 10 pictures at each temperature, increases with the aging time and reaches the maximum value at 4 h. Moreover, the highest percentage of α phase occurs at 617 °C. Another high volume fraction of α phase is at about 660 °C, which is near the “nose-temperature” in the TTT curve of Ti-5553 alloy. The volume fraction of α phase

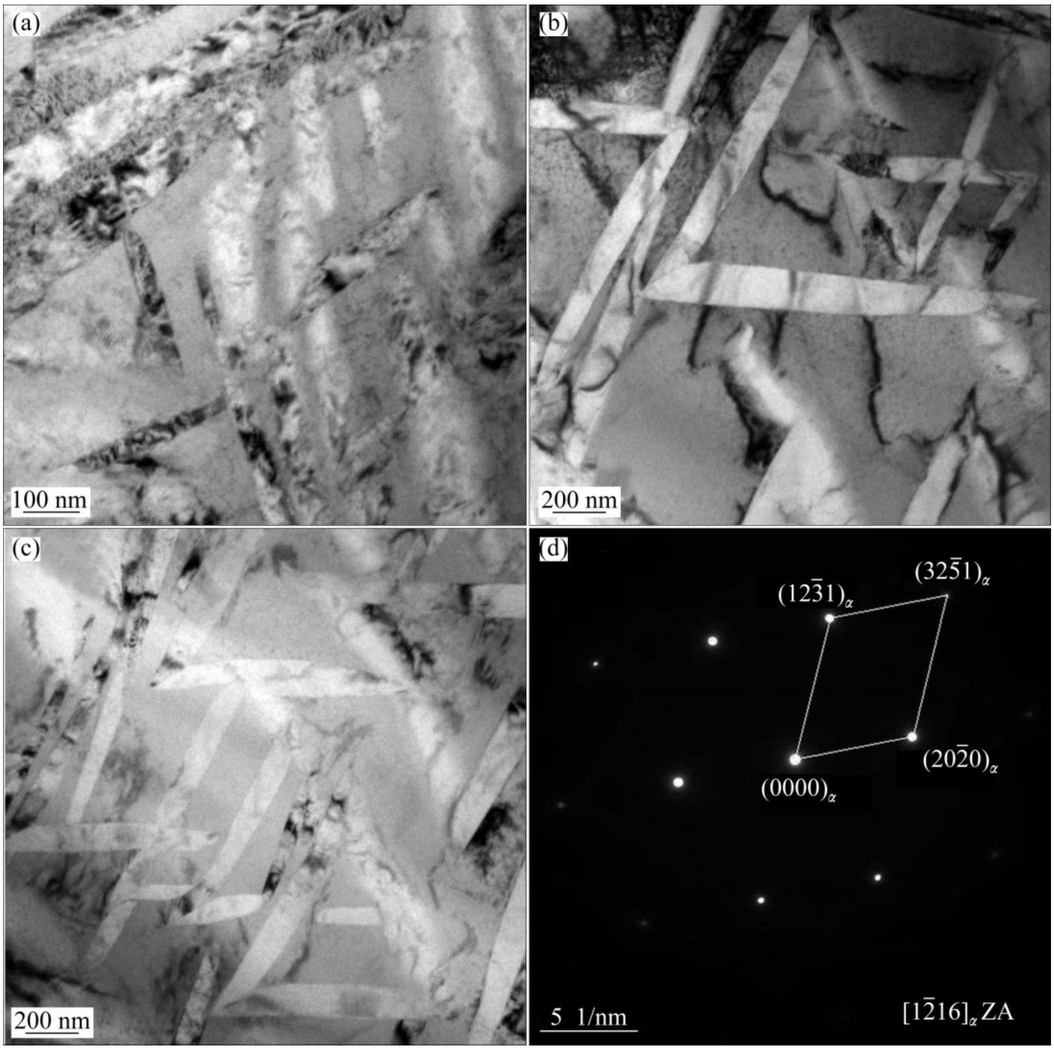

Fig. 4 TEM images of Ti-5553 alloy after heat treatment for 1 h: (a) 617 °C; (b) 640 °C; (c) 660 °C; (d) SAD pattern of α phase

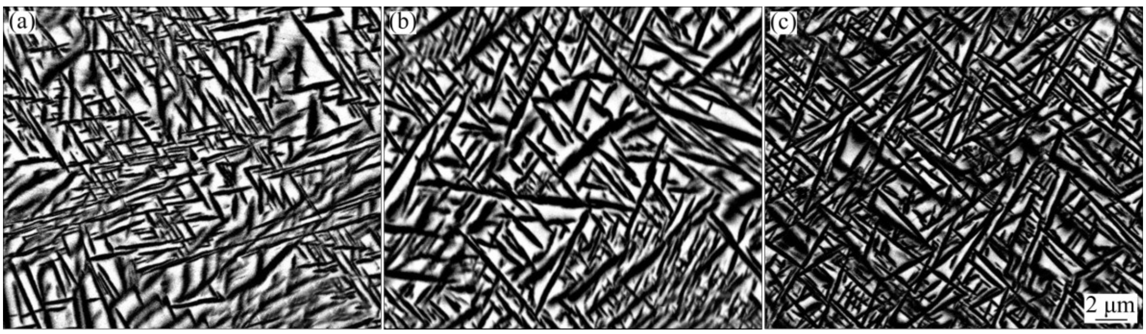

Fig. 5 Microstructures of Ti-5553 alloy aged at 640 °C for different time: (a) 30 min; (b) 1 h; (c) 4 h

reaches 54% at 617 °C and 51% at 660 °C when aging for 4 h.

3.3 Evolution of microstructures with cooling rate

In order to better illustrate the effect of the cooling rate on the precipitation of α phase at 617 °C, the end quenching test was performed, and the microstructures are shown in Fig. 7. Figures 7(a) and (c) show the microstructures of water quenched (WQ) and air cooled (AC) samples, respectively, and Fig. 7(b) presents that of the samples after the mixed cooling (MC) of water quenching and air cooling. All the samples show superfine α phase, and the volume fraction of α phase increases with decreasing the cooling rate. The XRD patterns in Fig. 8 also show the increase of α phase from Fig. 7(a) to Fig. 7(c). Figure 9 shows the morphology of

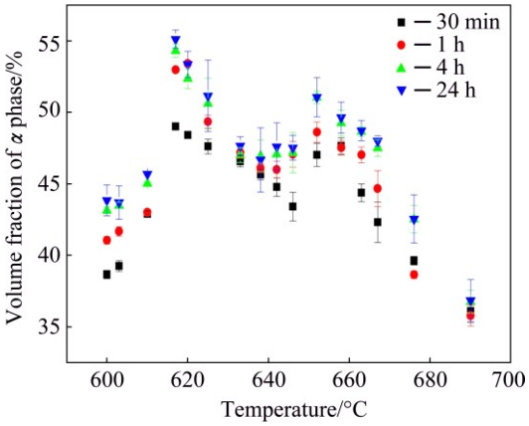

Fig. 6 Variation of volume fraction of α phase with aging temperature at different aging time

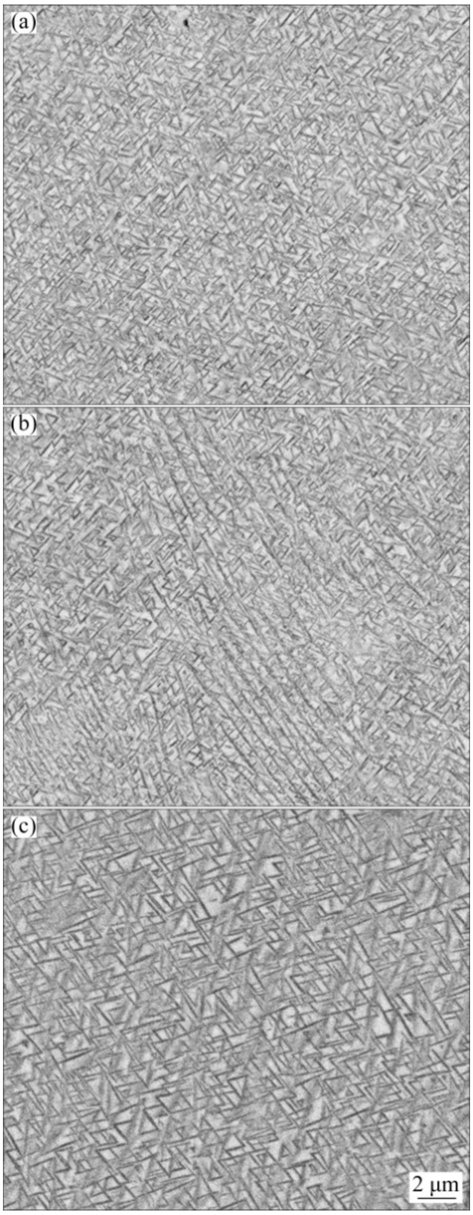

Fig. 7 Microstructures of Ti-5553 alloy after aging at 617 °C for 1 h and then cooling at different rates: (a) WQ; (b) MC; (c) AC

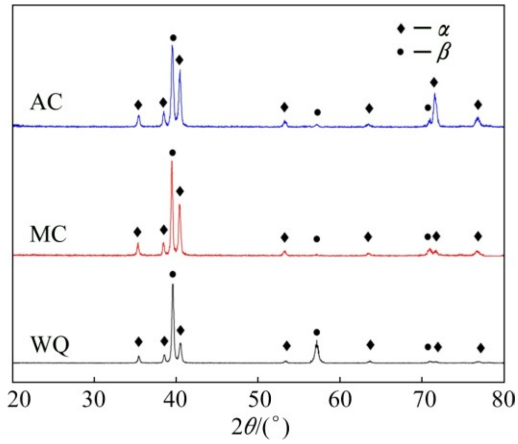

Fig. 8 XRD patterns of Ti-5553 alloy after aging at 617 °C for 1 h with different cooling rates

α phase precipitated in β matrix through WQ, MC and AC. Smaller α phase can be found in WQ and MC.

3.4 Mechanical properties

The nanoindentation measurement results in Fig. 10 show that the value of microhardness reaches the highest value of HV 548 at 617 °C. Moreover, another peak value of the microhardness can be seen at the nose-temperature of TTT curve of 660 °C, about HV 487. Along with the extending of aging time, the hardness value increases slightly.

4 Discussion

The new high throughput method utilized in this work can successfully and efficiently achieve the temperature gradient on a single sample. The accurate temperatures, which remain steady during the heat preservation process, can be obtained directly from seven thermoelectric couples on the sample as follows: 600, 617, 635, 651, 666, 681 and 705 °C. Moreover, the exact temperature corresponding to the areas between two thermoelectric couples on the sample can be calculated by Eq. (4), which is proportional to the inverse of the cross-sectional area of the sample. So, the temperature of any position on the sample can be calculated. Then, the phase transformation temperature and the corresponding evolution of microstructures can be systematically studied. By this method, the pseudo-spinodal decomposition temperature of Ti-5553 alloy is determined to be (617±1) °C, according to the fine morphology and the drastic increase in the volume fraction of α phase. The accurate pseudo-spinodal decomposition temperature shows obvious range owing to the relative wide region containing the special pseudo-spinodal decomposition microstructure, and the temperature range is approximately ±1 °C, which is

Fig. 9 Microstructures of Ti-5553 alloy aging at 617 °C for 1 h with different cooling rates: (a) WQ ; (b) MC; (c) AC

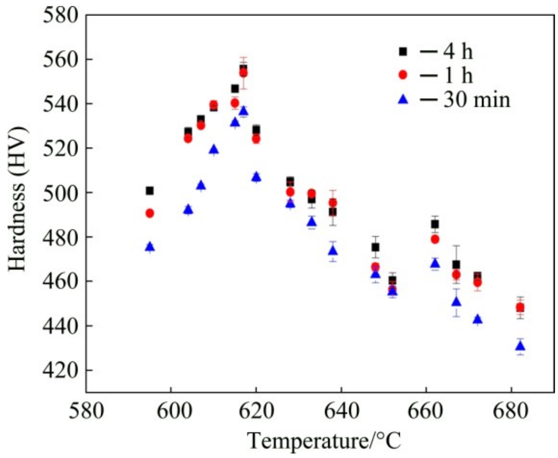

Fig. 10 Variation of Vickers hardness with aging temperature at different aging time

calculated by the width of the region. However, NAG et al [8] found that the pseudo-spinodal decomposition temperature of Ti-5553 alloy is about 600 °C through three aging experiments between 600 and 700 °C for 30 min, and the length of α phase is in the range of 400 nm−5 μm. Because of the temperature range of the pseudo-spinodal decomposition, the sample aged at 600 °C only shows the very beginning of the formation of α phase. Only the fine α phase and drastic increase in its volume fraction can be used to determine the exact temperature. In this work, the temperature of the sample is continuous, so the exact phase transformation temperature can be determined exactly by the microstructural observations.

Previous studies showed that the formation of ω phase may provide heterogeneous nucleation sites for the precipitation of α phase [18−24]. By this way, the fine-scale distribution of α phase can be affected by the dispersed ω phase. Previous research shows that ω phase in Ti alloy formed during fast cooling can be detected by XRD [25]. However, the XRD pattern in Fig. 2(b) does not show the peaks of the ω phase, which indicates the absence of the ω phase during cooling process. However, the ω phase can also exist when aging temperature over 300 °C [19], and the ω-solvus has been determined to be about 400 °C for Ti-5553 alloy, but heating at a relative fast rate (>20 °C /min) can avoid the formation of ω precipitates [23]. Hence, the precipitation of α phase during the pseudo-spinodal decomposition in this work occurs by the direct decomposition of β phase. When aging at the pseudo-spinodal decomposition temperature, a little fluctuation of compositions may change the difference of Gibbs free energy between α and β phases, resulting in the transformation of β to α [6]. A large amount of α/β interfaces can block the motion of the dislocations, and then strengthen the matrix [24,26−29]. Besides, the submicron α phase can also strengthen the β phase by the Orowan mechanism [30]. Thus, the highest microhardness was obtained after the heat treatment at the pseudo-spinodal decomposition temperature where the size of α phase is the finest and the volume fraction is the largest. In addition, when aging at 660 °C, the nose temperature of the TTT curve of Ti-5553 alloy, the nucleation rate of α phase also markedly increases. So, the value of microhardness reaches another peak at 660 °C.

5 Conclusions

1) Through the high throughput heat treatment, the pseudo-spinodal decomposition temperature of Ti-5553 alloy is measured to be (617±1) °C.

2) The length of α phase after the pseudo-spinodal decomposition is about 300 nm. The longer aging time or the slower cooling rate does not affect the size of α phase, but increases the volume fraction.

3) The small size and high volume fraction of α phase obtained by pseudo-spinodal decomposition leads to the highest microhardness.

References

[1] QIN Dong-yang, LU Ya-feng, LIU Qian, ZHENG Li, ZHOU Lian. Transgranular shearing introduced brittlement of Ti−5Al−5V−5Mo−3Cr alloy with full lamellar structure at room temperature [J]. Materials Science and Engineering A, 2013, 572: 19−24.

[2] KAR S K, ATASI G, NISHANT F, AMIT B. Quantitative microstructural characterization of a near beta Ti alloy, Ti-5553 under different processing conditions [J]. Materials Characterization, 2013, 81: 37−48.

[3] ZONG Ying-ying, HUANG Shu-hui, GUO Bin, SHAN De-bin. In situ study of phase transformations in Ti−6Al−4V−xH alloys [J]. Transactions of Nonferrous Metals Society of China, 2015, 25(9): 2901−2911.

[4] MOHAMMED M T, ZAHID A K, GEETHA. Effect of thermo-mechanical processing on microstructure and electrochemical behavior of Ti−Nb−Zr−V new metastable β titanium biomedical alloy [J]. Transactions of Nonferrous Metals Society of China, 2015, 25(3): 759−769.

[5] IVASISHIN O M, MARKOVSKY P E, SEMIATIN S L, WARD C H. Aging response of coarse- and fine-grained β titanium alloys [J]. Materials Science and Engineering A, 2005, 405(1−2): 296−305.

[6] NI Yong, RAO Wei-feng, ARMEN G K. Pseudospinodal mode of decomposition in films and formation of chessboard-like nanostructure [J]. Nano Letters, 2009, 9: 3275−3281.

[7] BOYNE A, WANG D, SHI R P, ZHENG Y, BEHERA A, NAG S, TILEY J S, FRASER H L, BANERJEE R, WANG Y. Pseudospinodal mechanism for fine α/β microstructures in β-Ti alloys [J]. Acta Materialia, 2014, 64: 188−197.

[8] NAG S, ZHENG Y, WILLIAMS R E A, DEVARAJ A, BOYNE A, WANG Y, COLLINS P C, VISWANATHAN G B, TILEY J S, MUDDLE B C, BANERJEE R, FRASER H L. Non-classical homogeneous precipitation mediated by compositional fluctuations in titanium alloys [J]. Acta Materialia, 2012, 60(18): 6247−6256.

[9] NI Y, KHACHAYURYAN A G. From chessboard tweed to chessboard nanowire structure during pseudospinodal decomposition [J]. Nature materials, 2009, 8(5): 410−414.

[10] LEROUX C, LOISEAU A, BRODDIN D, VANTENDELOO G. Electron microscopy study of the coherent two-phase mixtures L10+ L12, in Co−Pt alloys [J]. Journal of the Less Common Metals, 1991, 64(1): 57−82.

[11] BENDERSKY L A, BOETTINGER W J. Phase transformations in the $(Ti,Nb)_3Al$ section of the Ti−Al−Nb system. 2: Experimental TEM study of microstructures [J]. Acta Metallurgica et Materialia, 1994, 42: 2337−2352.

[12] YEO S, HORIBE Y, MORI S, TSENG C M, CHEN C H, KHACHATURYAN A G, ZHANG C L, CHEONG S W. Solid state self-assembly of nanocheckerboards [J]. Applied Physics Letters, 2006, 89(23): 233120.

[13] ZHANG C L, YEO S, HORIBE Y, CHOI Y J, GUHA S, CROFT M, CHEONG S W, MORI S. Coercivity and nanostructure in magnetic spinel $Mg(Mn,Fe)_2O_4$ [J]. Applied Physics Letters, 2007, 90(13): 479−566.

[14] GUITON B S, DAVIES P K. Nano-chessboard superlattices formed by spontaneous phase separation in oxides [J]. Nature Materials, 2007, 6(8): 586−591.

[15] AFONSO C R M, ALEIXO G T, RAMIREZ A J, CARAM R. Influence of cooling rate on microstructure of Ti−Nb alloy for orthopedic implants [J]. Materials Science and Engineering C, 2007, 27(4): 908−913.

[16] BU F Z, WANG X M, CHEN L, YANG S W, SHANG C J, MISAR R D K. Influence of cooling rate on the precipitation behavior in Ti−Nb−Mo microalloyed steels during continuous cooling and relationship to strength [J]. Materials Characterization, 2015, 102: 146−155.

[17] ZHENG Yu-feng. Nucleation mechanisms of refined alpha microstructure in beta titanium alloys [D]. Ohio: The Ohio State University, 2013.

[18] DEHGHAN M A, RIAN J D. Development of α-phase morphologies during low temperature isothermal heat treatment of a Ti−5Al−5Mo−5V−3Cr alloy [J]. Materials Science and Engineering A, 2011, 528(3): 1833−1839.

[19] NAG S, BANERJEE R, SRINIVASAN R, HWANG J Y, HARPER M, FRASER H L. ω-Assisted nucleation and growth of α precipitates in the Ti−5Al−5Mo−5V−3Cr−0.5Fe β titanium alloy [J]. Acta Materialia, 2009, 57(7): 2136−2147.

[20] DEVARAJ A, NAG S, SRINIVASAN R, WILLIAMS R E A, BANERJEE S, BANERJEE R, FRASER H L. Experimental evidence of concurrent compositional and structural instabilities leading to ω precipitation in titanium–molybdenum alloys [J]. Acta Materialia, 2012, 60(2): 596−609.

[21] HUANG Jun, WANG Zhi-rui, ZHOU Jie. Cyclic deformation response of β-Annealed Ti−5Al−5V−5Mo−3Cr alloy under compressive loading conditions [J]. Metallurgical and Materials Transactions A, 2011, 42(9): 2868−2880.

[22] CHEN Jing, XIAO Wen-long, DARGUSCH M S, MA Chao-li. The dependence of isothermal ω precipitation on the quenching rate in a metastable β-Ti alloy [J]. Scientific Reports, 2015, 5: 14632.

[23] JONES N G, DASHWOOD R J, JACKSON M, DYE D. β phase decomposition in Ti−5Al−5Mo−5V−3Cr [J]. Acta Materialia, 2009, 57(13): 3830−3839.

[24] SUN Zhi-chao, GUO Shuang-shuang, YANG He. Nucleation and growth mechanism of α-lamellae of Ti alloy TA15 cooling from an $\alpha+\beta$ phase field [J]. Acta Materialia, 2013, 61(6): 2057−2064.

[25] ZHANG Wei-dong, LIU Yong, WU Hong, SONG Min, ZHANG Tuo-yang, LAN Xiao-dong, YAO Tian-hang. Elastic modulus of phases in Ti−Mo alloys [J]. Materials Characterization, 2015, 106: 302−307.

[26] FAN J K, LI J S, KOU H C, HUA K, TANG B. The interrelationship of fracture toughness and microstructure in a new near β titanium alloy Ti−7Mo−3Nb−3Cr−3Al [J]. Materials Characterization, 2014, 96: 93−99.

[27] PRASAD R R, SHANKAR A, SINGH A K, MANDAL R K. Surface hardness behaviour of Ti−Al−Mo alloys [J]. Bulletin of Materials Science, 2008, 31(4): 687−691.

[28] NIINOMI M, KOBAYASHI T. Fracture characteristics analysis related to the microstructures in titanium alloys [J]. Materials Science and Engineering A, 1996, 213(1): 16−24.

[29] ZHANG Qiang, CHEN Jing, TAN Hua, LIN Xin, HUANG Wei-dong.

Microstructure evolution and mechanical properties of laser additive manufactured Ti−5Al−2Sn−2Zr−4Mo−4Cr alloy [J]. Transactions of Nonferrous Metals Society of China, 2016, 26(8): 2058−2066.

[30] ZHANG Z, CHEN D L. Contribution of Orowan strengthening effect in particulate-reinforced metal matrix nanocomposites [J]. Materials Science and Engineering A, 2008, 483−484: 148−152.

连续温度梯度热处理 Ti−5Al−5Mo−5V−3Cr 合金的显微组织演变与力学性能

徐圣航，刘 咏，刘 彬，王 鑫，陈智星

中南大学 粉末冶金国家重点实验室，长沙 410083

摘 要：采用一种新型高通量实验方法，实现对 Ti-5553 合金(Ti−5Al−5Mo−5V−3Cr，质量分数，%)在 600~700 °C 范围内的连续温度梯度热处理。实验通过对圆台形样品进行直流电加热，由于截面面积不同而导致电流热效应不同，从而使样品表面温度呈梯度变化。采用端淬实验实现 Ti-5553 合金的连续冷却速率变化，研究合金在不同热处理条件下的显微组织演变和力学性能。结果表明：Ti-5553 合金的伪调幅分解温度为(617±1) °C，析出的 α 相尺寸在 300 nm 左右；合金在伪调幅分解温度下时效 4 h 达到最高的硬度。因此，这种高通量方法能够快速准确地判断合金中相转变温度以及相应的组织转变。

关键词：Ti−5Al−5Mo−5V−3Cr 合金；高通量实验方法；伪调幅分解；温度梯度；显微组织；力学性能

(Edited by Wei-ping CHEN)